Comparative studies of powder flow predictions using milligrams of powder for identifying powder flow issues

Tong Deng [a,*], Vivek Garg [a], Laura Pereira Diaz [b,c], Daniel Markl [b,c], Cameron Brown [b,c], Alastair Florence [b,c], Michael S.A. Bradley [a]

[a] *Wolfson Centre for Bulk Solids Handling Technology, Faculty of Engineering & Science, University of Greenwich, Central Avenue, Chatham ME4 4TB, UK*
[b] *Strathclyde Institute of Pharmacy and Biomedical Sciences, University of Strathclyde, Glasgow G4 0RE, UK*
[c] *EPSRC Future Continuous Manufacturing and Advanced Crystallisation Research Hub, Glasgow G1 1RD, UK*

ARTICLE INFO

ABSTRACT

Characterising powder flowability can be challenging when sample quantity is insufficient for a conventional shear cell test, especially in the pharmaceutical industry, where the cost of the active pharmaceutical ingredient (API) used is expensive at an early stage in the drug product development. A previous study demonstrated that powder flowability could be predicted based on powder physical properties and cohesiveness using a small quantity of powder samples (50 mg), but it remained an open question regarding the accuracy of the prediction compared to that measured using industry-standard shear cell testers and its potential to substitute the existing testers.

In this study, 16 pharmaceutical powders were selected for a detailed comparative study of the predictive model. The flowability of the powders was predicted using a Bond number and given consolidation stresses, σ_1, coupled with the model, where the Bond number represents powder cohesiveness. Compared to the measurements using a Powder Flow Tester (Brookfield) and an FT4 (Freeman Technology) Powder Rheometer shear cell tester, the results showed a good agreement between the predictions and the measurements (<22 % difference) from the two shear cell testers with different consolidation stresses, especially for cohesive materials. The model correctly predicts the class of flowability for 14 and 12 of the 16 powders for the PFT and the FT4, respectively. The study demonstrated that the prediction method of powder flowability using a small sample (50 mg) could substitute a standard shear cell test (>15 g) if the available amount of sample is small.

1. Introduction

In pharmaceutical manufacturing processes, powder flow property is a crucial bulk property for ensuring the processes are well controlled, and a consistent drug product quality can be maintained (Schulze, 2008; Alyami, et al., 2017). Powder flow can particularly impact the content uniformity of active pharmaceutical ingredients (APIs) between drug products. A drug formulation is often designed without considering issues in the process caused by the poor flowability of the raw materials (Lawrence, 2008). This may lead to severe variations in the content uniformity leading to out-of-specification products and consequential financial losses (Krantz, et al., 2009). Powder flowability needs to be well understood early in the drug product development to make well-informed decisions on the manufacturing route (e.g., direct compression vs wet granulation) and the formulation (e.g., drug loading).

However, the assessment of powder flow requires a significant amount of powder samples to measure it using common shear cell tests accurately (15 g minimum for one test). Due to the influential factors involved in various ingredients with different physical properties and selection options in different formulations, the sample quantity required for shear cell tests can be significant up to kilograms. However, the quantity of a new drug substance available at an early stage is typically on the scale of grams, which limits the tests that can be performed and lead to risks in the decision-making of the manufacturing route and formulation.

Assessing powder flowability using only a small amount of powder would be greatly advantageous in the early stages of drug product development (Barjat, et al., 2021). A new technique (Garg, et al., 2021) developed at the Wolfson Centre can predict powder flowability only based on material's physical properties and cohesiveness which are

---

represented by measuring the Bond Number using milligrams of powders (Deng, et al., 2021). The method assumes that a small sample of powders (typically < 100 mg) contains enough particles to represent distributions of sizes, shapes, and contact orientations, which can result in measurements that capture the stochastic effects of particle morphology, surface chemistry and bulk behaviour. The model has been applied for many ingredients successfully (Garg, et al., 2021), but it remains unknown how well the predictions agree with results from different types of shear cell tests which are commonly used in industry.

This study aims to compare the predictions of flow functions for a wide range of common pharmaceutical materials selected to the measurements using two types of commonly used shear cell testers. In the study, 16 pharmaceutical powders with a wide range of particle size and solid density are used for inferring Bond number by measuring particle adhesion on a mechanical surface energy tester. With the Bond number, powder flow functions are predicted using the model previously developed (Garg, et al., 2021) and compared to that measured on the two types of shear cell testers, i.e., Powder Flow Tester (PFT, Brookfield) and an FT4 (Freeman Technology) Powder Rheometer. This comparison enables the assessment of the suitability of the prediction model for accurately identifying flow problems using a small quantity of sample material (50 mg).

2. Powder flow and prediction model

Powder flow is defined as the dynamic movement of particles among neighbouring particles or along a surface of containers (Peleg, 1977). Powder flowability is the ability of granular solids and powders to flow (Ganesan, et al., 2008). The flow of powders can be very complex, which depends on many physical properties of the powder, particle contacts and initial dynamic conditions of solids (Garg, et al., 2018). Powder flowability is restricted by the material's physical properties and the consolidation stress (Prescott and Barnum, 2000). Therefore, it remains a challenge to fully quantify a powder's flowability by a single test that accounts for all the influential factors.

2.1. Powder flow characterisations

Powder flow of bulk solids can be assessed in many ways, including the angle of repose, angle of internal friction, cohesion, adhesion, compressibility, *etc.* (Ganesan, et al., 2008). However, each method has its own limitations and physical meanings. The influential factors on powder flow can be material physical properties or dynamic influences (Goh, et al., 2018). It is easy to understand the influences of the material properties, such as size distributions and shape differences, which can cause the powder to flow easily or not. For the dynamic influences, it is difficult to define them clearly as they may be subjected to the particle and bulk properties, for example, friction coefficients between particles that are strongly influenced by the particle size (Garg, et al., 2018).

The flowability of powders is commonly assessed using flow functions defined as a yield locus plot of failure shear stress versus normal stress applied for a given consolidating stress, as shown in Eq. (1). Shear cell tests are the most popular and established methods to measure powder flowability. Jenike (Jenike, 1964) was the first to create a fundamental method for powder flow characterisation using the principles of plastic failure with the Mohr-Coulomb failure criteria (Thomson, 1997). This led to the development of several common types of testers in the past (Schwedes, 2002, Ganesan, et al., 2008). In the pharmaceutical industry, the existing characterisation methods of powder flowability have a clear challenge when significant sample powders (from several grams to tens of grams) are required (Prescott and Barnum, 2000; Hassanpour, et al., 2019). This is not a problem if the powders are available, but it can be a challenge at the stage of pre-clinical trials or the development of the formulation (Cun, et al., 2021). For manufacturing purposes, the flowability of the formulated blends is essential to know.

Table 1
A list of the materials studied and suppliers (Material codes are used in the analysis, and corresponding names and grades can be found in the table).

No	Code	Material	Grade	Supplier
1.	MCC-101	Microcrystalline Cellulose (MCC)	Avicel PH-101	Dupont
2.	MCC-102	Microcrystalline Cellulose (MCC)	Avicel PH-102	Dupont
3.	CCS	Croscarmellose sodium	GMO	Dupont
4.	MAN-D	Mannitol	D-mannitol	Foremost
5.	LAC	Lactose monohydrate	Lactose monohydrate, NF	Foremost
6.	CPD	Calcium phosphate dibasic	GL21117	Sigma-Aldrich
7.	HPMC	Hydroxypropyl methylcellulose	Benecel K100M	Ashland
8.	LAN	Co-processed excipient with anhydrous lactose and glyceryl monostearate	Lubritose AN	Kerry
9.	L-MCC	Co-processed excipient with MCC and glyceryl monostearate	Lubritose MCC	Kerry
10.	L-PB	Pre-lubricated blend of anhydrous lactose, MCC, and glyceryl monostearate	Lubritose PB	Kerry
11.	L-DC	Hydroxypropyl methylcellulose	Methocel DC2	Dow
12.	IBU-50	Ibuprofen	Ibuprofen 50	BASF
13.	IBU-70	Ibuprofen	Ibuprofen 70	BASF
14.	SOL	Polyvinyl caprolactam-polyvinyl acetate-polyethene glycol graft co-polymer	Soluplus	BASF
15.	MGST	Magnesium stearate	Dry coated	Roquette
16.	MAN	Mannitol	Pearlitol 300 DC	Roquette

$$\text{Flow Function Coefficient}(ffc) = \frac{\text{major principal stress}, \sigma_1}{\text{unconfined yield strength}, \sigma_c} \qquad (1)$$

2.2. Prediction model based on particle adhesion

Instead of performing a measurement using shear cell tests, powder flow properties can be predicted using material physical properties such as particle size and powder cohesiveness. In the previous study (Garg, et al., 2021), a prediction model of powder flowability was introduced based on the correlations between powder flowability and cohesiveness of powders, where a Bond number was used for representing powder cohesiveness.

A linear relationship was found between the Bond number (*Bo*) and the flow functions for different levels of consolidation stresses based on a simple judgement of 'highly cohesive powder would be hard to flow'. This is expressed in Eq. (2) with the slope of the linear relationship and the intercept of the equations as a function of consolidation stress levels (σ_1), as shown in Eqs. (3) and (4).

$$1/ffc = m(Bo) + c \qquad (2)$$

where

$$m = a_1 \ln(\sigma_1) + b_1 \qquad (3)$$

$$c = a_2(\sigma_1)^{b_2} \qquad (4)$$

a_1, a_2, b_1 and b_2 are constants taken from the previous study as −0.020, −0.420, 0.117 and −0.073, respectively. Therefore, the model for flowability prediction can be expressed as:

$$1/ffc = [-0.020\ln(\sigma_1) + 0.117](Bo) - 0.420(\sigma_1)^{-0.073} \qquad (5)$$

Once a Bond number for a powder is determined (see section 3.3.2), the flow function of the powder can be predicted at given consolidation

stress, σ_1. The σ_c values can be obtained with a known flowability using Eq. (1), if σ_1 is given.

3. Materials and methods

3.1. Materials

Sixteen pharmaceutical materials covering various excipients and drug substances were investigated, as shown in Table 1, which covered a wide range of flow properties.

3.2. Material characterisations

3.2.1. Particle size

Particle size distributions (PSDs) of the sample materials were measured by the laser diffraction method (Mastersizer 2000, Malvern Panalytical, ltd., Malvern, UK) with a dry dispersion unit. A sample of approximately 10 g was used for 5 repeats measured at 2 bars air pressure and 60 % feed rate. An averaged result from all measurements was used for the study.

Particle size span defined in Eq. (6) was calculated using the PSDs measured to demonstrate the particle size range that can significantly influence the powder flow.

$$S_{span} = (D_{90} - D_{10})/D_{50} \tag{6}$$

where D_{50} represents the size in diameter where the percentage of powder is less or equal to 50 % in volume. D_{10} and D_{90} are the sizes where 10 % and 90 % of the powder are below the size, respectively.

3.2.2. Solid density

True particle density was measured using a gas pycnometer (Ultra-pyc 1200e, Quantachrome Instruments, Florida, USA) with nitrogen gas. The measurement was repeated five times and an average value was taken with a standard deviation of about 0.05 % of the measurement.

3.2.3. Scanning Electron Microscope (SEM)

The SEM images were captured on JSM-5510 Scanning Electron Microscope (JEOL (Europe) BV, Zaventem, Belgium). The images of the powders were taken on Aluminium stubs using double-sided carbon tape and coated with a 5 mm layer of gold/palladium (Au: Pd ¼ 80:20). The instrument was operated at an accelerating voltage of 15 kV, and the images were taken at a magnification of 1000.

3.3. Powder flowability methods

3.3.1. Shear cell tests for powder flowability

A powder flow tester (PFT) (Brookfield Engineering Laboratories, Inc., Middleboro, MA, USA) and an FT4 Powder Rheometer (Freeman Technology, ltd., Tewkesbury, UK) were used to determine the powder flowability experimentally.

The PFT is based on the principles of Jenike's methodology (Jenike, 1964) to determine the powder flow function defined in Eq. (1). The tester consists of an annular shear cell of which the volume of the cell usually is 263 cm^3 or 43 cm^3 for a small cell. Sample powder is loaded into the cell, and consolidation stress is applied to the sample via the lid. Once a desired consolidation stress level is reached, a shear force is then applied to the cell. A top knifed lid is mounted for conducting the shear cell measurement (flow function). A torque force generated through the powder to the lid is recorded, which calculates the Mohr's circle and the unconfined failure strength at the consolidation stress level.

In the study of powder flow functions measured using the PFT, axial and torsional speeds for the PFT were 1.0 mm/s and 1 rev/hr, respectively. The tests were carried out at ambient temperature (~20–25 °C) and humidity (40–60 % RH). The equipment was automated with the 'Powder Flow Pro software, which provided the data of yield locus and flow functions as a function of major principal consolidation stress. For the current tests, a range of applied uniaxial normal stresses was applied from about 1 to 10 kPa.

An FT4 Powder Rheometer was used to analyse the flow function coefficient (*ffc*) of the materials. A split cell (10 ml in volume with a diameter of 25 mm) was selected to run the measurements. The first step was the conditioning cycle carried out by a 23.5 mm stainless steel blade that rotates clockwise downwards and upwards throughout the powder, followed by the compaction step at major principal consolidation stress of 9 kPa. Once the powder was compacted, the excess powder above the split of the vessel was removed, and the shear cell test measurement was conducted. The shear cell blade moved downwards to the powder bed. This process provided the powder's yield locus, and by fitting Mohr's circles, the major principal stress and the unconfined yield strength can be calculated, which gives the flow function coefficient as shown in Eq. (1).
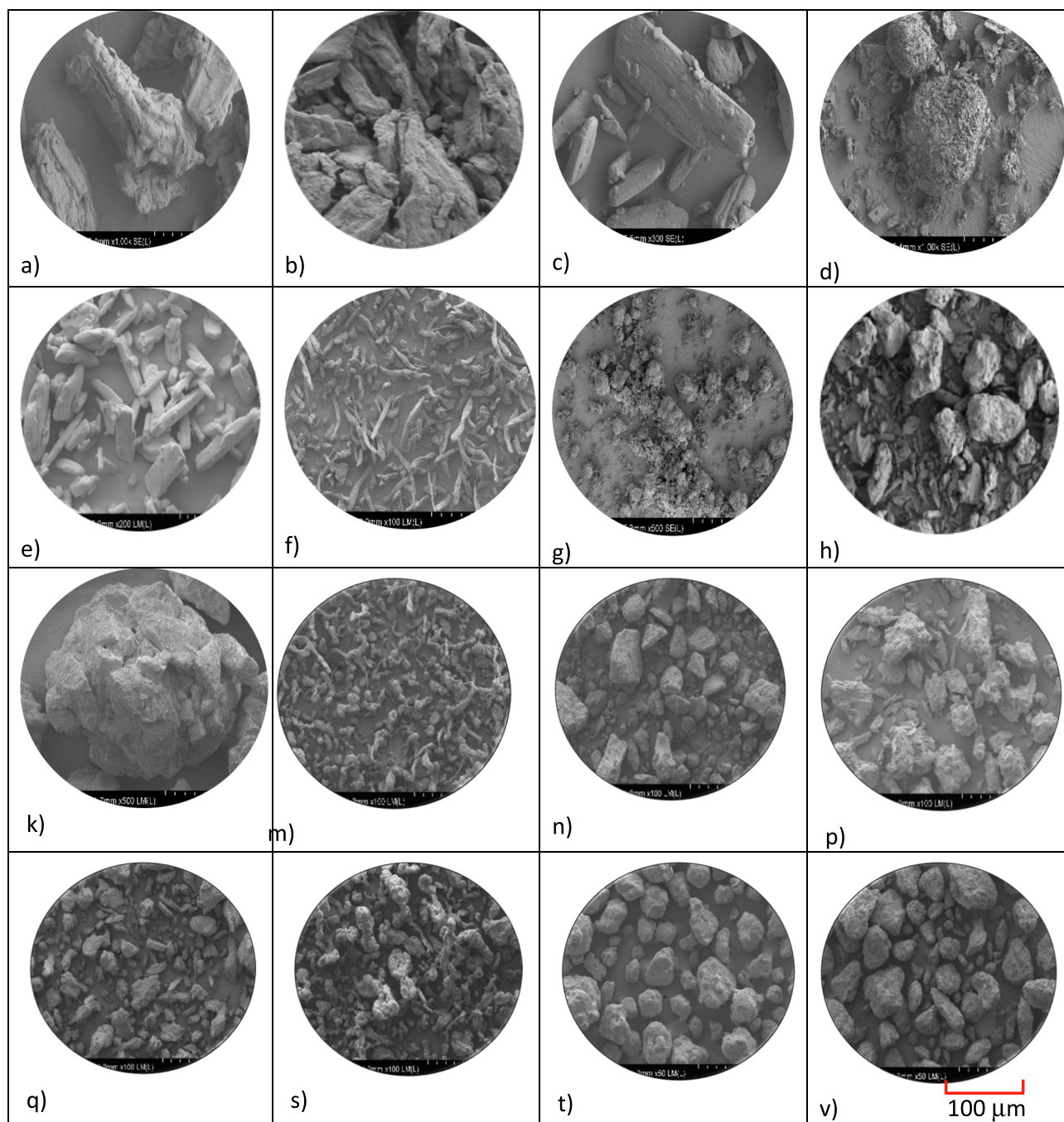
3.3.2. Mechanical surface energy tester

The Bond number is used for the prediction of powder flowability as given in Eq. (5) (Capece, et al., 2015). The Bond number (*Bo*) is defined as a ratio of particle adhesion force, F_{ad}, to particle gravity force, F_g, for cohesive particles, as shown in Eq. (7) (Deng, et al., 2021).

$$Bo = F_{ad}/F_g = F_{ad}/(mg) \tag{7}$$

where

$$F_{ad} = \frac{H_a D^*}{12 z_0^2} \tag{8}$$

z_0 is the separation distance between two surfaces, H_a is the Hamaker constant that depends on the material properties and D^* is the equivalent diameter of the particles. In this study, a mechanical surface energy tester was used to measure the particle adhesion force for determining the Bond number. In the measurements, a standard disc made of glass was used as a substrate surface instead of a powdered substrate due to its small influence on the results (Deng, et al., 2021). In the tests, about 50 mg of a sample powder was dispersed onto the substrate using an air expansion disperser operated at a pressure of 1.5 bar. The sampled substrate was weighed to measure the mass of the dispersed sample powder using a digital balance (accuracy of 0.1 mg). The substrate disc was fitted onto a carriage that could slide down along a guide rod under gravity and stop against a metal buffer to create a measured deceleration of the particles. The mass of the powders detached from the disc was measured using a digital balance. The acceleration and the mass (50 %

Table 2
Material physical properties of the materials studied.

Code	Particle Size (µm)			Size Span	Solid Density (kg/m^3)
	D_{10}	D_{50}	D_{90}	S_{span}	
MCC-101	22.1	59.1	128.8	1.8	1562
MCC-102	34.0	122.7	264.7	1.9	1562
CCS	16.0	40.0	88.0	1.8	1585
MAN-D	5.3	44.8	170.8	3.7	1462
LAC	17.8	67.0	84.5	1.0	1544
CPD	1.1	14.8	34.3	2.2	3581
HPMC	32.3	112.4	1277.4	11.1	1596
LAN	17.7	128.2	350.7	2.6	1608
L-MCC	76.9	180.5	403.9	1.8	1670
L-PB	36.3	160.9	416.1	2.4	1663
L-DC	45.9	119.6	321.4	2.3	1460
IBU-50	5.3	26. 6	75.8	2.7	1110
IBU-70	3.7	23.0	80.0	3.3	1110
SOL	202.4	322.3	505.2	0.9	1208
MGST	1.5	5.96	18.4	2.8	1600
MAN	50.5	265.0	485.5	1.6	1584

Fig. 1. SEM images of the materials studied: a) MCC-101, b) MAN-D, c) IBU-70, d) MGST, e) IBU-50, f) CCS, g) CPD, h) MCC-102, k) LAC, m) HPMC, n) LAN, p) L-MCC, q) L-PB, s) L-DC, t) SOL and v) MAN. Magnification for all materials was kept constant, as shown in Fig. 1 v).

detached from the total dispersed particles) were used for the calculation of the F_{ad} and the Bo in Eq. (7) at the particle size measured by the Mastersizer 2000.

4. Results and discussion

With the 16 materials, the flowability of the samples is predicted using the model shown in Eq. (5) based on the Bond numbers measured. The predictions of powder flow functions are compared to the measurements using two types of shear cell testers. Based on the comparison, the feasibility of predicting powder flow properties using a small quantity of sample powder (50 mg) is discussed as a substitution for a standard shear cell test.

4.1. Material properties

Characteristics of the materials studied are given in Table 2. Particle size percentile values (volumetric percentage) for the materials are also shown in the table with other physical properties, including size span calculated and solid particle density measured.

SEM images of the materials are given in Fig. 1, indicating that the particles vary significantly in size and shape, ranging from spherical-like (SOL, Fig. 1 (t)) to needle-like particles (IBU-50, Fig. 1 (e)). The SEM images further show that some powders contain agglomerates, such as MAN-D (Fig. 1 (b)). In general, the smaller the particle size, the stronger particle adhesion forces that cause agglomeration.
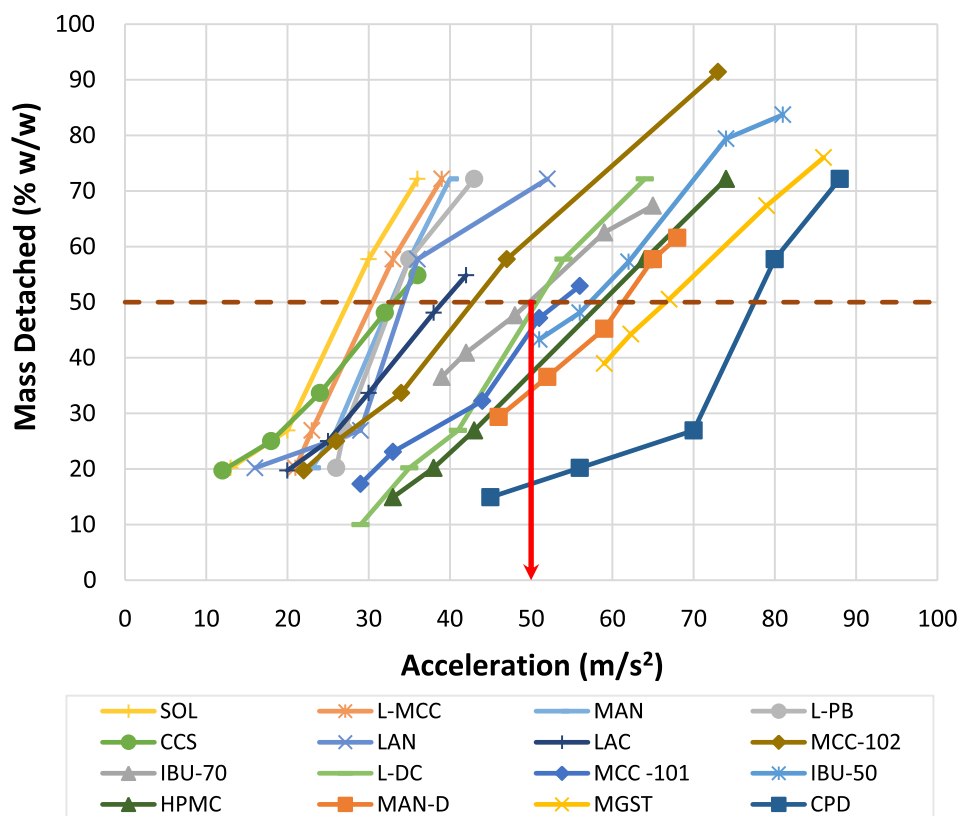
Fig. 2. The mass proportions detached from the particles deposited on a standard substrate at different decelerations for the 16 sample powders. The horizontal dashed line represents the 50% mass detached, and the vertical red arrow indicates the acceleration with the corresponding material at 50% mass detached. (For interpretation of the references to colour in this figure legend, the reader is referred to the web version of this article.)
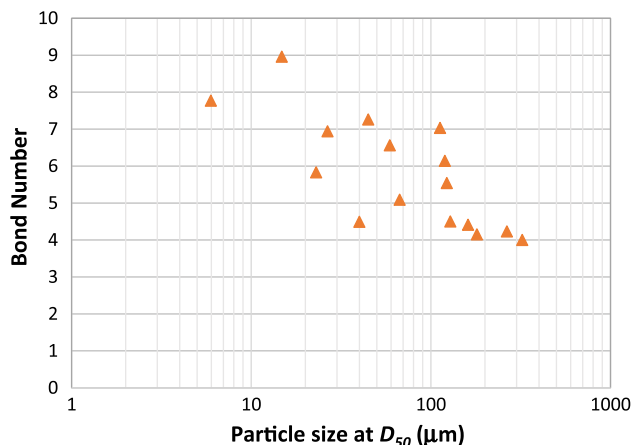

Fig. 3. The Bond numbers measured versus the size of D_{50} for the 16 sample powders.

Table 3
Particle Bond numbers for the sample materials at the size of D_{50}.

Sample code	Particle Size, D_{50} (µm)	Accelerations (m/s²)	Bond Number
MCC-101	59.1	54.52 ± 1.06	6.56
MAN-D	44.8	61.34 ± 1.78	7.26
IBU-70	23.0	47.34 ± 1.95	5.83
MGST	6.0	66.35 ± 2.55	7.77
IBU-50	26.6	58.20 ± 2.63	6.94
LAC	67.0	40.12 ± 7.95	5.09
CCS	40.0	34.16 ± 1.93	4.49
MCC-102	122.7	44.50 ± 0.43	5.54
CPD	14.8	78.00 ± 1.01	8.96
HPMC	112.4	59.10 ± 1.95	7.03
SOL	322.3	29.40 ± 1.44	4.00
MAN	265.0	31.65 ± 0.75	4.23
L-DC	119.6	50.37 ± 0.47	6.14
L-PB	161.0	33.42 ± 5.03	4.41
L-MCC	180.5	30.87 ± 0.48	4.15
LAN	128.2	34.30 ± 0.48	4.50

4.2. Particle adhesion and Bond numbers

Particle adhesion of the 16 powders was measured using the mechanical surface energy tester. The accelerations measured for all sample powders are presented in Fig. 2, which shows the mass percentage of the detached material over the total material deposited versus the acceleration needed for the detachment.

In Fig. 2, the proportion of the material detached from the substrate surface increases proportionally with an increased acceleration applied. Using the acceleration value measured at the 50 % mass detached and the mass of the detached particles (whose particle size is equivalent to the D_{50} by mass), the adhesion force of the is calculated by multiplying

the mass and the acceleration. The Bond numbers for the 16 materials are shown in Fig. 3, following Eq. (7).

The particle size of D_{50}, the accelerations measured for the 50 % mass detached and the Bond numbers for the 16 samples powders are given in Table 3. In general, a higher Bond number means that the powder is more cohesive, and the particle size is smaller. The materials with a similar particle size may have a different Bond number because of their different cohesiveness of the materials.

4.3. Predictions of the flowability using the Bond numbers

The powder flowability of the powders is predicted using the model shown in Eq. (5) and the Bond number measured. Taking the model and
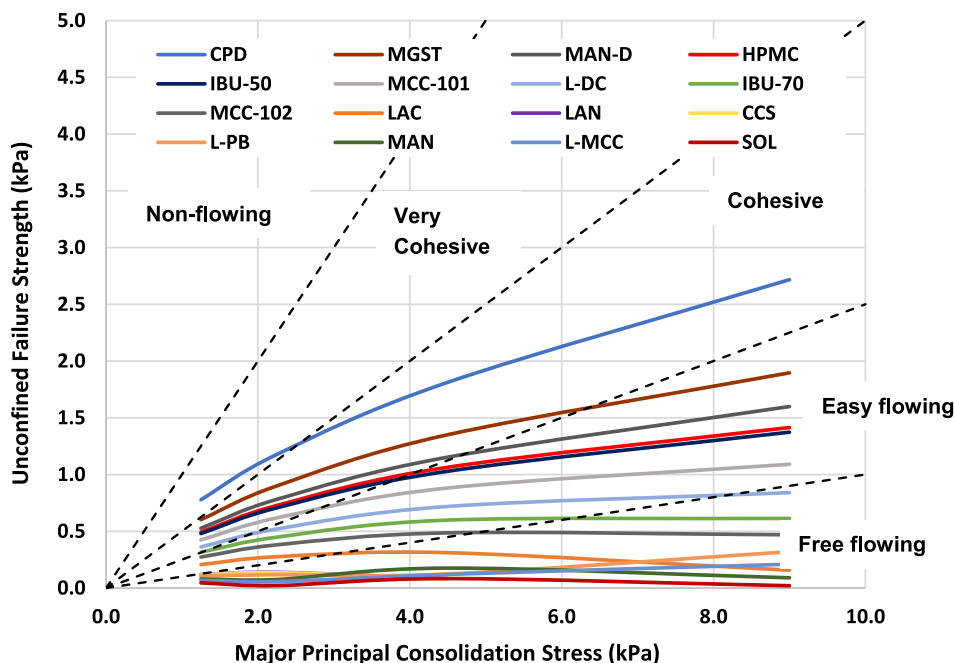
Fig. 4. Predicted flow functions at four consolidation stresses of 1.25 kPa, 2.25 kPa 4.5 kPa and 9.0 kPa for the 16 sample powders.

Table 4
Aggregated Bond numbers and the flow function predictions for the materials.

S. No.	Materials	Particle Size (μm)			Solid Density (kg/m³)	Bond Number	Predicted Flow Function
		D_{10}	D_{50}	D_{90}		Bo	ff (at 1000 Pa)
1	MCC-101	22.1	59.1	128.8	1562	6.56	2.95
2	MAN-D	5.3	44.8	170.8	1462	7.26	2.37
3	IBU-70	3.7	23.0	80.0	1110	5.83	3.95
4	MGST	1.5	5.96	18.4	1600	7.77	2.07
5	IBU-50	5.3	26. 6	75.8	1110	6.94	2.60
6	LAC	17.8	67.0	84.5	1544	5.09	6.05
7	CCS	16.0	40.0	88.0	1585	4.49	10.60
8	MCC-102	34.0	122.7	264.7	1562	5.54	4.50
9	CPD	1.1	14.8	34.3	3581	8.96	1.60
10	HPMC	32.3	112.4	1277.4	1596	7.03	2.51
11	LAN	17.7	128.2	350.7	1608	4.5	10.40
12	L-MCC	76.9	180.5	403.9	1670	4.15	17.56
13	L-PB	36.3	160.9	416.1	1663	4.41	10.89
14	L-DC	45.9	119.6	321.4	1460	6.14	3.40
15	SOL	202.4	322.3	505.2	1208	4.00	26.98
16	MAN	50.5	265.0	485.5	1584	4.23	15.12

four consolidation stresses at 1.25, 2.25, 4.5 and 9.0 kPa, the flow functions for the powders can be predicted as shown in Fig. 4.

The predictions of the flow functions at 1 kPa consolidation stress of the 16 materials can also be found in Table 4 with corresponding material properties and the Bond numbers.

4.4. Results of flowability from the shear cell tests

The powder flowability of the sample powders was measured using PFT and FT4 Powder Rheometer shear cell tester. Because the shear cell test is a widely used method for evaluating powder flowability in industry, the experimental results from two types of shear cell testers were used for comparison between the experiments and the predictions.

The sample powders in Table 1 were used in the shear cell tests covering a wide range of flowability, particle properties and cohesiveness. The flow functions measured on the PFT for the samples are depicted in Fig. 5, which shows the powders are classified in various flow regimes, from free-flowing to cohesive. In the tests, five consolidation stresses were used for the measurements, i.e., from about 5 kPa to

30 kPa. The flow functions of the powders were then obtained using Eq. (1).

With the measured data on the PFT shear cell tester (Fig. 5), the flow functions can be interpreted at different consolidation stresses in the range of up to 30 kPa. At a given major principal consolidation stress, a flow function coefficient can be calculated.

The flow functions of the sample powders were measured at major principal consolidation stress of 9 kPa on the FT4 Powder Rheometer (Fig. 6). With the failure strength measured, the flow functions of the powders using the FT4 Powder Rheometer can be obtained by Eq. (1). It is noted that for the FT4 Powder Rheometer, only one consolidation stress was used.

4.5. Comparison between the predictions and the measurements

With the results measured on the PFT and FT4 shear cell testers shown in Figs. 5 and 6, the predictions at the same consolidation stress are shown in Table 5.

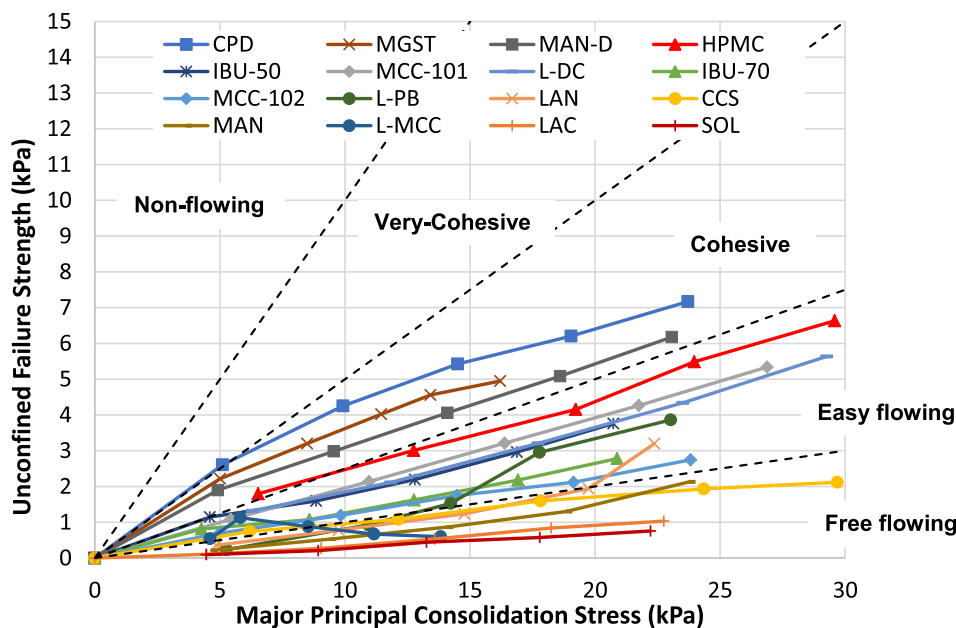With the data, the measured flow functions on the testers are directly

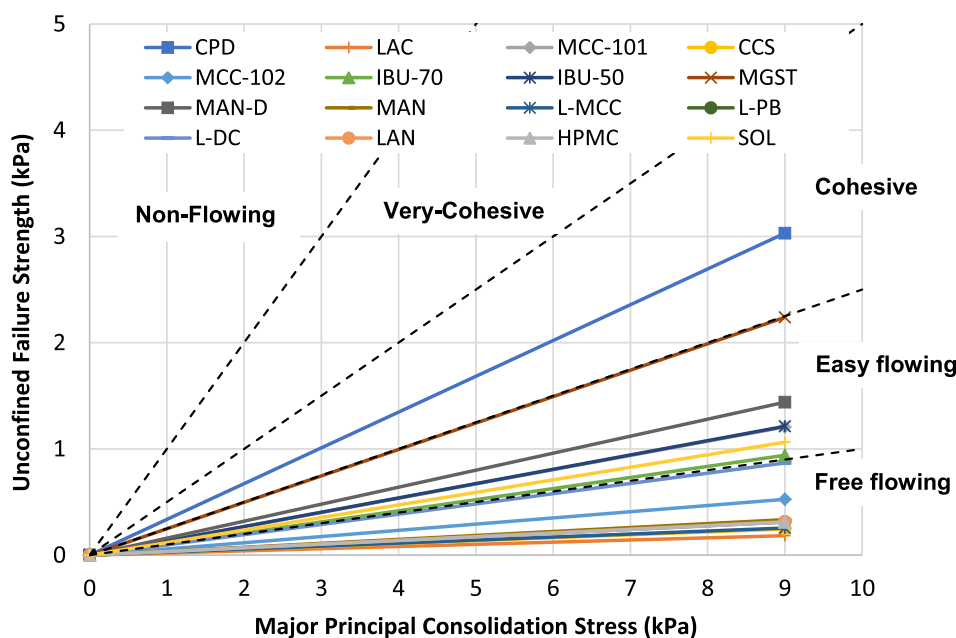**Fig. 5.** Instantaneous flow functions of the sample powders measured using a PFT shear cell tester.

Fig. 6. Instantaneous flow functions of the sample powders measured using an FT4 Powder Rheometer.

compared to the predictions at the same consolidation stress. A ratio of the experimental *ffc* to the predicted *ffc* ($R = ffc_{(expt)} / ffc_{(predicted)}$) is calculated for all samples measured on the PFT at the consolidation stress of 4.5 kPa and the FT4 tester at the consolidation stress of 9.0 kPa. The ratios for all the sample materials are shown in Fig. 7.

Fig. 7 shows that most predictions of powder flow functions using the model are in good agreement with the measured values for both shear testers (PFT at 4.5 kPa and FT4 at 9.0 kPa). The ratios of the experiments and the predictions are very close to 1, which means the predictions are in good agreement with the measurements. However, this analysis indicated that there are two outliers: one is the LAC for PFT at 4.5 kPa, and the other one is HPMC for FT4 at 9.0 kPa. To evaluate the outliers, the ratios of the experimental *ffc* to the predicted *ffc* for both testers have been analysed using Cook's distance test and Difference in Fits (DFFIT).

The statistical analysis is shown in Figs. 8 and 9, which clearly indicates the Cook's distances for HPMC (FT4 tester) and LAC (PFT tester) are significantly larger than for the other sample materials. Although the values of Cook's distance for HPMC (0.8) and LAC (0.6) are not significant (<1.0), the difference in fits for the HPMC and LAC is significant, and the values are bigger > 1.0 (6.1 for HMPC and 4.7 for LAC). If the outliers identified here are removed from the data, the averaged ratio for the PFT tester at the consolidation stress of 4.5 kPa is 0.81 ± 0.12 and 0.84 ± 0.22 for the FT4 tester at the consolidation stress of 9.0 kPa.

The averaged ratios of the experiments and the prediction for both testers show that, generally, the experimental measurements have smaller average ratios as compared to the predictions. Without the outliers, the model has about 18 % overprediction compared to the experiments. For the PFT tester, the averaged ratio has a low value

Table 5
Comparative results between the measurements (the PFT at 4.5 kPa and the FT4 tester at 9 kPa) and the flow function predictions for the materials.

Materials	Bond Number	Predicted Flow Function	Measured Flow Function (PFT)	Predicted Flow Function	Measured Flow Function (FT4)
	Bo	ff (at 4.5 kPa)	ff (at 4.5 kPa)	ff (at 9 kPa)	ff (at 9 kPa)
CPD	8.96	2.48	1.96	2.35	2.97
MGST	7.77	3.33	2.28	5.07	4.02
MAN-D	7.26	3.90	2.92	6.16	6.25
HPMC	7.03	4.23	3.47	6.36	28.94
IBU-50	6.94	4.37	4.01	7.13	7.42
L-DC	6.14	6.26	4.25	11.54	10.37
MCC-101	6.56	5.11	5.02	8.77	7.46
IBU-70	5.83	7.52	6.35	15.68	9.58
MCC-102	5.54	9.26	7.17	22.84	17.12
L-MCC	4.15	10.37	7.33	42.86	35.23
LAN	4.5	16.28	14.42	31.03	28.63
MAN	4.23	25.62	22.50	60.00	27.00
L-PB	4.41	36.44	31.38	28.13	28.84
CCS	4.49	57.33	34.13	69.23	36.63
LAC	5.09	14.46	42.50	78.26	49.19
SOL	4.00	54.11	56.60	8.82	8.47

Note: The table is classified into 4 groups from top to bottom using measured flow functions on the PFT, as very cohesive ($ffc < 2$), cohesive ($2 < ffc < 4$), easy-flowing ($4 < ffc < 10$) and free-flowing ($ffc > 10$).
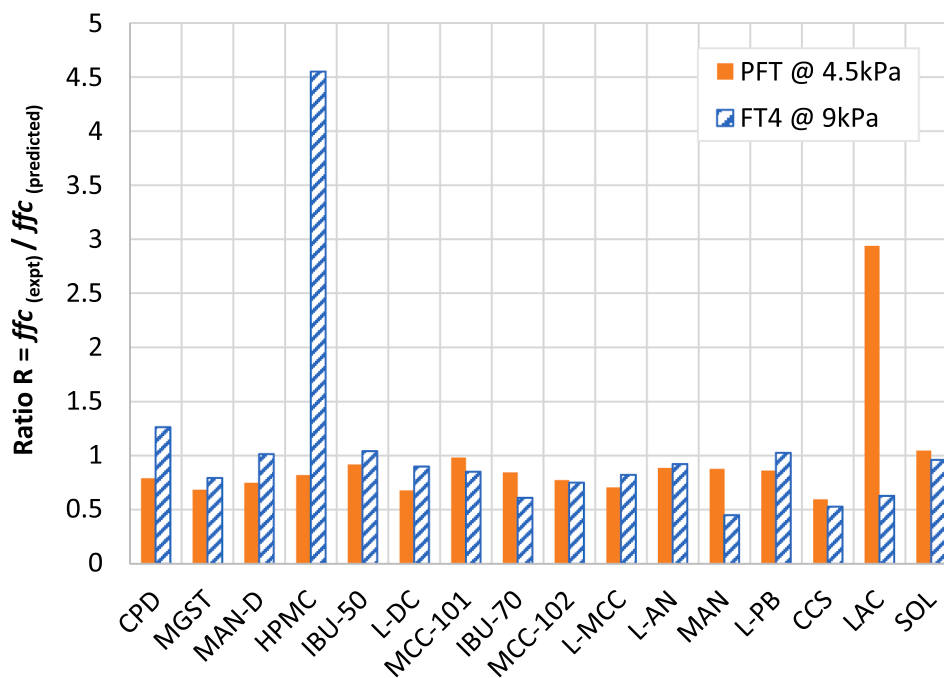

Fig. 7. Ratios of the experimental ffc to the predicted ffc on a PFT tester at 4.5 kPa and a FT4 tester at 9 kPa consolidation stresses for all the sample materials.

(0.81) and shows overprediction with low standard deviation of 0.12. For the FT4 tester, it shows less overprediction (the averaged ratio is 0.84), but a large standard deviation of 0.22 for the average.
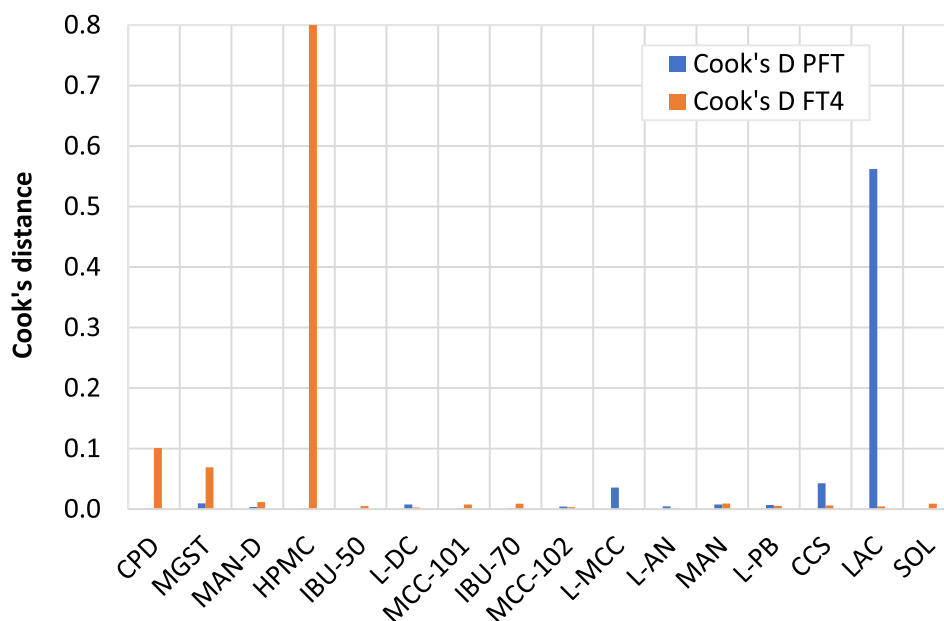
For the two testers, the ratios of the experimental ffc to the predicted ffc are directly compared (Fig. 10). The predictions appear uncorrelated with consolidation stress applied in the tests and the types of shear cell testers. If the outliers identified are excluded, all predictions are concentrated in a small area (in the red circle), which is close to 1. Taking the centre of the circle, it shows the average ratio is about 0.82

(about 18 % overprediction).

4.6. Discussion of the flow function predictions

The prediction model of Eq. (5) only requires two parameters in the calculation of a powder flow function: an aggregated Bond number and consolidation stresses (σ_1). With any consolidation stresses given, in principle, the flow function can be calculated using the Bond number. To measure the Bond number, only 50 mg is required, which is also

Fig. 8. Analysis of Cook's distance test for the ratios of the experimental *ffc* to the predicted *ffc* on the PFT tester at 4.5 kPa and the FT4 tester at 9 kPa consolidation stresses.
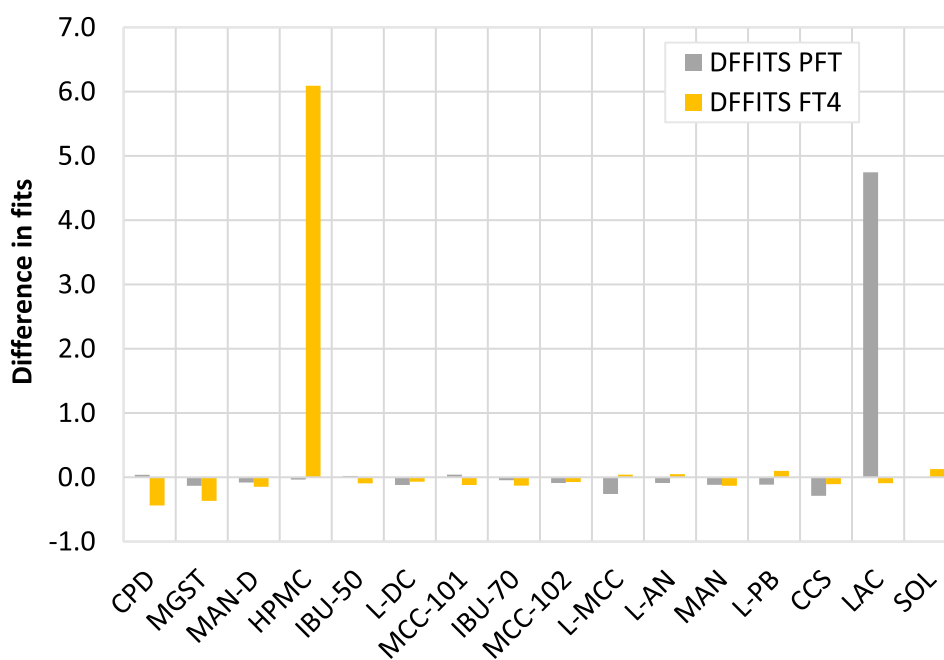
Fig. 9. Analysis of Difference in fits (DFFIT) for the ratios of the experimental *ffc* to the predicted *ffc* on the PFT tester at 4.5 kPa and the FT4 tester at 9 kPa consolidation stresses.

sufficient for the particle size measurement if a Malvern G3 Morphology is used. If using the laser diffraction method, more sample materials may be required (about 1 to 5 g). Therefore, the flow function of a powder can be predicted using as minimum as 50 mg of powder.

In contrast, to measure powder flow functions using a shear cell tester, the sample required is more significant. For a PFT tester, one test requires at least 20 g. For an FT4 shear cell tester, the sample needed for one test is about 15 g, which depends upon particle size and solid density. The sampling requirement is also a significant barrier in determining flow functions at an early stage in drug development. The unknown flow properties of an API and the formulations become high risk in the manufacturing process and can result in enormous waste and

huge financial losses if the flowability of the formulation is unforeseen poor, which is more likely to be a cohesive material.

The results in Figs. 7 and 9 indicate that the predictions are in good agreement with the experiments except for two cases. In general, the model shows an overprediction with relatively small errors with a standard deviation between 0.12 and 0.22. Over a wide range of powder flow functions, the model works well from free-flowing to cohesive materials. Excluding the outliers in the study, the results in Fig. 10 show that the model is promising for predictions of powder flow functions at varied consolidation stresses. However, the comparisons in Fig. 11 show that the model works better for cohesive materials (higher Bond numbers), where the predictions are close to the measurements. The
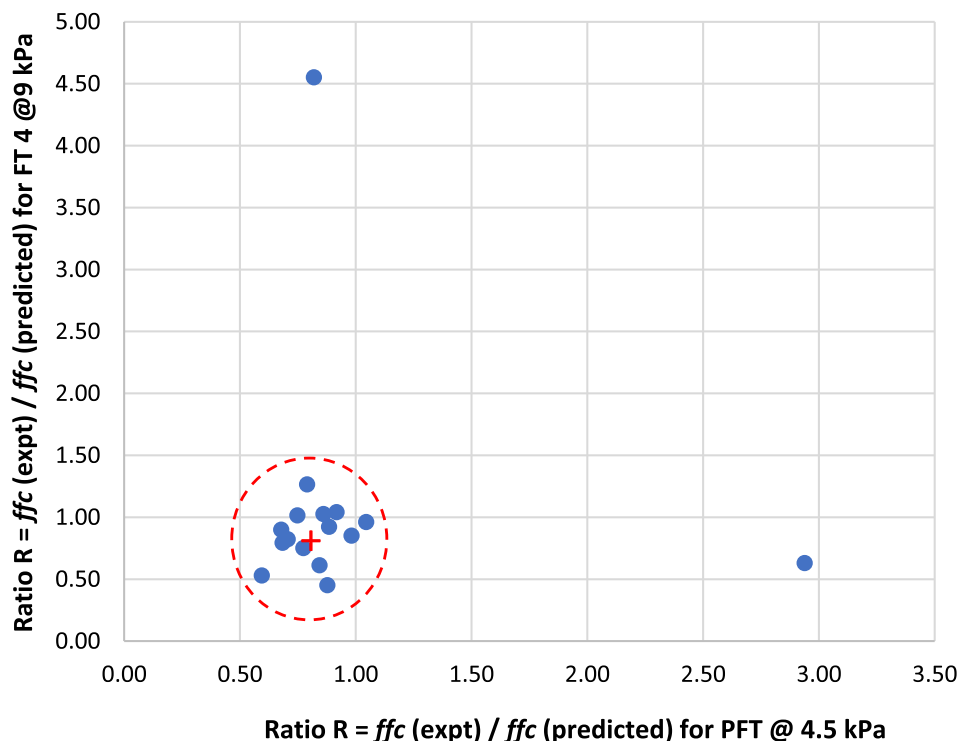
Fig. 10. Ratios of the experimental *ffc* to the predicted *ffc* on the PFT tester at 4.5 kPa consolidation stress versus the ratios on the FT4 tester at 9 kPa consolidation stress.
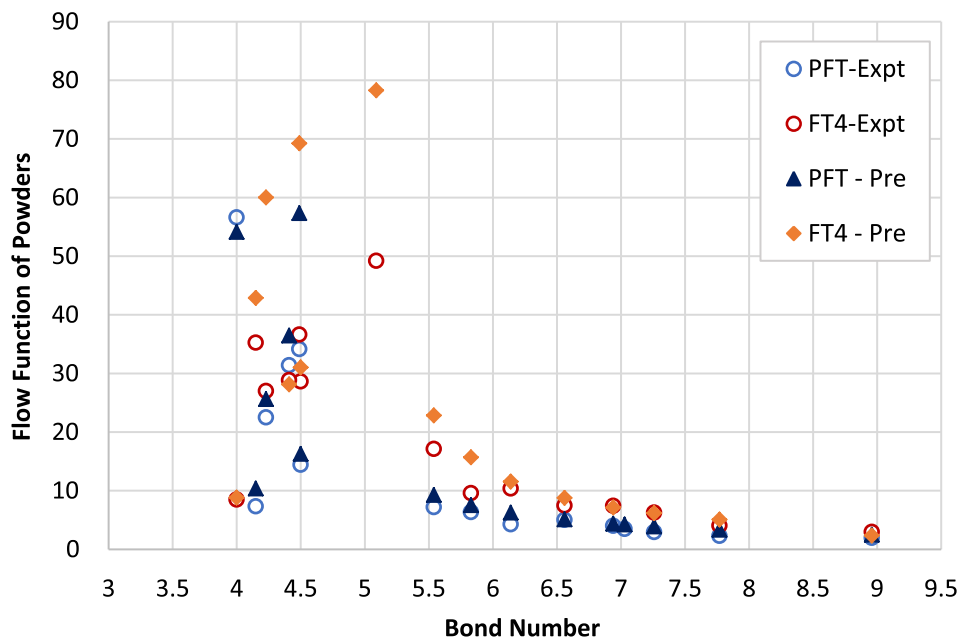

Fig. 11. Comparison between the experimental flow functions on a PFT tester at 4.5 kPa and a FT4 tester at 9 kPa and the predictions versus the corresponding Bond numbers.

model can still be applied for easy-flowing to free-flowing powders (Bond number between 4 and 5), although random errors can be larger. More extreme cases can be found in the tests on the FT4 tester compared to the PFT tester. In the case of cohesive powders (Bond number between 5.5 and 9), the predictive model works very well to substitute a shear cell test for powder flow function measurements.

5. Conclusions

Flow functions of 16 pharmaceutical powders were predicted using a model previously developed based on Bond numbers and the material properties. The results show that the predictions are in a good agreement with the measurements using annular shear cell testers (Powder Flow Tester, Brookfield and FT4 shear cell tester). The study also shows a very good agreement with both types of shear cell testers at different

consolidation stresses.

The statistical analysis revealed that the model works better for cohesive powders. For free-flowing materials, the model predictions deviate from the experimental results. Unsurprisingly, the prediction deviates from the measurements for free-flowing materials as the cohesiveness of powders is negligible. It is important to consider that the flowability of cohesive powders is significantly more relevant to the industry than free-flowing powders because of the different cohesive APIs involved. It can therefore be concluded that the mechanical surface energy testing coupled with the model in Eq. (5) delivers a better indication of the flowability in the range of powder properties relevant to the pharmaceutical industry. This study also indicates that the model has an overall overprediction of 18 %, compared to the experiments.

The predictive method developed demonstrates great potential for its application in the pharmaceutical industry. It makes a strong case to substitute a shear cell test when only a small amount of material is available. The predictive model can be used to benchmark formulations to identify a "window of acceptable flow function". It can further be applied to test "what-if" scenarios for blends in changing the size distribution of new APIs or adjusting the excipients to obtain favourable flow properties for manufacturing.

CRediT authorship contribution statement

Tong Deng: Writing – original draft, Writing – review & editing, Conceptualization, Investigation, Methodology, Funding acquisition, Project administration. **Vivek Garg:** Writing – original draft, Writing – review & editing, Conceptualization, Data curation, Investigation, Formal analysis, Validation. **Laura Pereira Diaz:** Investigation, Writing – review & editing. **Daniel Markl:** Writing – review & editing, Supervision, Project administration. **Cameron Brown:** Writing – review & editing, Supervision. **Alastair Florence:** Resources, Project administration. **Michael S.A. Bradley:** Supervision, Resources, Project administration.

Declaration of Competing Interest

The authors declare that they have no known competing financial interests or personal relationships that could have appeared to influence the work reported in this paper.

Data availability

Data will be made available on request.

Acknowledgement

References

Alyami, H., Dahmash, E., Bowen, J., Mohammed, A.R., 2017. An investigation into the effects of excipient particle size, blending techniques and processing parameters on the homogeneity and content uniformity of a blend containing low-dose model drug. PloS One, 12(6), e0178772.

Barjat, H., Checkley, S., Chitu, T., Dawson, N., Farshchi, A., Ferreira, A., Gamble, J., Leane, M., Mitchell, A., Morris, C., Pitt, K., Storey, R., Tahir, F., Tobyn, M., 2021. Demonstration of the feasibility of predicting the flow of pharmaceutically relevant powders from particle and bulk physical properties. J. Pharm. Innovation 16 (1), 181–196.

Capece, M., Ho, R., Strong, J., Gao, P., 2015. Prediction of powder flow performance using a multi-component granular Bond number. Powder Technol. 286, 561–571.

Cun, D., Zhang, C., Bera, H., Yang, M., 2021. Particle engineering principles and technologies for pharmaceutical biologics. Adv. Drug Deliv. Rev. 174, 140–167.

Deng, T., Garg, V., Bradley, M.S.A., 2021. A study of particle adhesion for cohesive powders using a novel mechanical surface energy tester. Powder Technol. 391, 46–56.

Ganesan, V., Rosentrater, K.A., Muthukumarappan, K., 2008. Flowability and handling characteristics of bulk solids and powders–a review with implications for DDGS. Biosyst. Eng. 101 (4), 425–435.

Garg, V., Mallick, S.S., García-Trinanes, P., Berry, R.J., 2018. An investigation into the flowability of fine powders used in pharmaceutical industries. Powder Technol. 336, 375–382.

Garg, V., Deng, T., Bradley, M.S., 2021. A new method for assessing powder flowability based on physical properties and cohesiveness of particles using a small quantity of samples. Powder Technol. 395, 708–719.

Goh, H.P., Heng, P.W.S., Liew, C.V., 2018. Comparative evaluation of powder flow parameters with reference to particle size and shape. Int. J. Pharm. 547 (1–2), 133–141.

Hassanpour, A., Hare, C., Pasha, M. (Eds.), 2019. Powder flow: Theory, characterisation and application. Royal Society of Chemistry.

Jenike, A.W., 1964. Storage and flow of solids. Bulletin No. 123, Utah Engineering Station. Bulletin of the University of Utah, USA.

Krantz, M., Zhang, H., Zhu, J., 2009. Characterisation of powder flow: Static and dynamic testing. Powder Technol. 194 (3), 239–245.

Lawrence, X.Y., 2008. Pharmaceutical quality by design: product and process development, understanding, and control. Pharm. Res. 25 (4), 781–791.

Peleg, M., 1977. Flowability of food powders and methods for its evaluation—a review. J. Food Process Eng 1 (4), 303–328.

Prescott, J.K., Barnum, R.A., 2000. On powder flowability. Pharm. Technol. 24 (10), 60–85.

Schulze, D., 2008. Powders and bulk solids. Behaviour, characterisation, storage and flow. Springer, p. 22.

Schwedes, J., 2002. Consolidation and flow of cohesive bulk solids. Chem. Eng. Sci. 57 (2), 287–294.

Thomson, F.M., 1997. Storage and flow of particulate solids. In Handbook of Powder Science & Technology. In: Fayed, M.E., Otten, L. (Eds.), Handbook of Powder Science & Technology. Springer US, Boston, MA, pp. 389–486.